Transp Porous Med (2008) 72:1–24
DOI 10.1007/s11242-007-9132-5

CO_2 injection into saline carbonate aquifer formations I: laboratory investigation

Omer Izgec · Birol Demiral · Henri Bertin · Serhat Akin

Received: 13 July 2005 / Accepted: 2 April 2007 / Published online: 12 May 2007

Abstract Although there are a number of mathematical modeling studies for carbon dioxide (CO_2) injection into aquifer formations, experimental studies are limited and most studies focus on injection into sandstone reservoirs as opposed to carbonate ones. This study presents the results of computerized tomography (CT) monitored laboratory experiments to analyze permeability and porosity changes as well as to characterize relevant chemical reactions associated with injection and storage of CO_2 in carbonate formations. CT monitored experiments are designed to model fast near well bore flow and slow reservoir flows. Highly heterogeneous cores drilled from a carbonate aquifer formation located in South East Turkey were used during the experiments. Porosity changes along the core plugs and the corresponding permeability changes are reported for different CO_2 injection rates and different salt concentrations of formation water. It was observed that either a permeability increase or a permeability reduction can be obtained. The trend of change in rock properties is very case dependent because it is related to distribution of pores, brine composition and thermodynamic conditions. As the salt concentration decreases, porosity and the permeability decreases are less pronounced. Calcite deposition is mainly influenced by orientation, with horizontal flow resulting in larger calcite deposition compared to vertical flow.

Keywords Carbon dioxide injection in carbonates · Geological sequestration · Permeability and porosity change

O. Izgec · B. Demiral · S. Akin (✉)
Petroleum and Natural Gas Engineering Department,
Middle East Technical University,
Inonu Bulvari, 06531 Ankara, Turkey
e-mail: serhat@metu.edu.tr

H. Bertin
Laboratoire TREFLE,
Esplanade des Arts et Métiers,
33405 Talence Cedex, France

1 Introduction

Carbon dioxide sequestration can be defined as the capture and secure storage of CO_2 that would have otherwise been emitted into or remained in the atmosphere (Bachu and Adams 2003; Pruess and Xu 2001). This approach aims to keep CO_2 emissions produced by human activities from reaching the atmosphere by capturing and diverting them to secure storage. CO_2 is sequestered in geological formations by three mechanisms: solubility trapping through dissolution in the formation water (Gunter et al. 1997; Reichle et al. 1999), mineral trapping through geochemical reactions with the aquifer fluids and rocks (Gunter et al. 1997; McPherson and Lichtner 2001; Goldberg et al. 2001), and hydrodynamic trapping of CO_2 plume (Bachu and Adams 2003; Reichle et al. 1999). These mechanisms lead to storage of CO_2 as free-phase gas in pore spaces, dissolution in formation water and CO_2 converted to rock matrix. Deep saline aquifers in sedimentary basins are possible sites for sequestration of CO_2. Brine formations are the most common fluid reservoirs in the subsurface, and more importantly large-volume formations are available in sedimentary basins that are widely spread around the world.

Flow systems that involve water, CO_2 and dissolved ions have been extensively studied in geothermal reservoir engineering. The geothermal work mostly addresses higher temperatures and lower CO_2 partial pressures than would be encountered in aquifer disposal of CO_2. Some of it involves not only multiphase flow but also chemical interactions between reservoir fluids and rocks (Izgec et al. 2005a). Injection of CO_2 into aquifers includes a variety of strongly coupled physical and chemical processes such as multiphase flow, solution–dissolution kinetics, solute transport, hydrodynamic instabilities due to displacement of brine with less viscous CO_2 (viscous fingering), and upward movement of CO_2 due to gravity override (Reichle et al. 1999). Reactions among the formation rock, the aquifer fluid and CO_2 may lead to change in the formation porosity and permeability, thus the storage capacity of the formation. Although there are plenty of numerical modeling studies (e.g., Doughty and Pruess 2004; Kumar et al. 2005; Hovorka et al. 2006) and a number of semi-analytical and analytical studies (Saripalli and McGrail 2002; Nordbotten et al. 2004) related to flow and transport during injection of CO_2 in geological formations, as well as numerical studies including geochemical reactions (e.g., Gunter et al. 1993; Pruess et al. 2003; Johnson et al. 2004; Nghiem et al. 2004), experimental studies are limited and most studies focus on sandstone aquifers as opposed to carbonate ones. Through the injection of CO_2 in carbonate deep saline aquifers, some changes in rock properties are expected. Changes in the rock porosity and permeability result from dissolution of rock minerals, transportation and precipitation. Continuous dissolution of reactant minerals alters the concentration of aquifer fluid, thus at later times leading to precipitation of product phases. While dissolution of rock minerals increases the formation porosity and permeability, precipitation of those minerals decreases the formation porosity and permeability (Izgec et al. 2005a, b, c).

At the CO_2 front where CO_2 is dissolved in water, minerals such as calcite may dissolve readily, leading to an increase in porosity and permeability along the flow path. This leads to a higher flow rate and increased dissolution, forming what is known as wormholes. It is also known from various field applications of enhanced oil recovery that CO_2 injection reduces injectivity in some cases (Ross et al. 1982) and increases permeability near injection wells in others, such as in carbonate reservoirs.

For a carbonate system kinetically controlled reactions can be defined as (Omole and Osoba 1983; Snoeyink and Jenkins 1980):

$$H_2O + CO_2 + CaCO_3 \leftrightarrow Ca(HCO_3)_2 \tag{1}$$

In general, atmospheric or subsurface CO_2 dissolves in water and generates a weak carbonic acid, H_2CO_3, which subsequently dissociates into HCO_3^- and CO_3^{2-} according to reaction steps given as:

$$CO_{2(gas)} \leftrightarrow CO_{2(aq)} \tag{2}$$

$$CO_{2(aq)} + H_2O \leftrightarrow H_2CO_{3(aq)} \tag{3}$$

$$H_2CO_{3(aq)} \leftrightarrow HCO_3^- + H^+ \tag{4}$$

$$HCO_3^- \leftrightarrow CO_3^{2-} + H^+ \tag{5}$$

The dissolved bicarbonate species react with divalent cations to precipitate carbonate minerals. Formation of Ca, Mg and Fe (II) carbonates are expected to be the primary means by which CO_2 is immobilized (Gunter et al. 1997).

$$HCO_3^- + Ca^{2+} \leftrightarrow CaCO_3 + H^+ \tag{6}$$

$$HCO_3^- + Mg^{2+} \leftrightarrow MgCO_3 + H^+ \tag{7}$$

$$HCO_3^- + Fe^{2+} \leftrightarrow FeCO_3 + H^+ \tag{8}$$

Mechanisms by which a precipitate reduces permeability include mineral precipitation on the pore walls due to attractive forces between the particles and the surfaces of the pores, individual particles blocking pore throats, and several particles bridging across a pore throat (Pruess and Xu 2001). In a carbonate formation, a major cause of reduction in porosity and permeability is precipitation of $CaCO_3$ and NaCl. Pressure drop along the flow path affects the precipitation rate, thus leading to variations in rock properties by changing the amount of substances that is dissolved. Assuming there is Darcian and incompressible flow in the porous media, there is a linear relationship between pressure drop and distance in the direction of flow if the rock is homogeneous. Considering this relationship and solute transport concept, it is expected that permeability increases in the near well bore region and then gradually decreases in the flow direction (Omole and Osoba 1983). Permeability decline caused by mineral precipitation in the porous bed can reach upto 90% of the initial permeability, depending on solution composition, initial permeability, temperature and flow rate and solution injection period (Moghadasi et al. 2005). On the other hand some researchers reported increase in the permeability of dolomite cores by 3.5–5% after similar CO_2 treatments, (Omole and Osoba 1983) while a reduction in permeability was observed in other experiments.

The relevant dimensionless parameters for the dissolution and deposition process are the Peclet, *Pe*, and Damkohler, *Da*, numbers (c.f., Bekri et al. 1995; Bhat and Kovscek 1999). The Peclet number is the ratio of convection speed to characteristic diffusive velocity, while the Damkohler number is the ratio of characteristic residence time or fluid motion time scale to characteristic reaction time. Zhang and Kang (2004) found that a large Damkohler number ($Da \gg 1$) corresponds to very rapid chemical reaction in comparison to all other processes. On the other hand, small Damkohler number ($Da \ll 1$) corresponds to very slow chemical reaction in comparison to all other processes. At high *Pe* and *PeDa* product, wormholes are formed and permeability increases greatly due to the dissolution process. At low *Pe* and high *PeDa* numbers, reactions mainly occur at the inlet boundary, resulting in near inlet dissolution and the slowest increase of the permeability in the dissolution process. At moderate *Pe* and *PeDa* numbers, reactions are generally non-uniform, with more in the upstream and

less in the downstream. At very small *PeDa* number, dissolution and precipitation are highly uniform in space, and these two processes can be approximately reversed by each other.

Assuming first order reactions, *Pe* and *Da* numbers can be obtained using the following expressions:

$$Pe = \frac{vd}{D} \tag{9}$$

$$Da = \frac{(1-\phi)\,\alpha L \kappa}{v} \tag{10}$$

where v is a characteristic velocity taken here as the mean interstitial velocity, d and L are characteristic dimensions, ϕ is porosity, D is the solute diffusivity, α is surface area ratio of the mineral, and κ is a first-order rate constant. The characteristic dimension in *Pe* is appropriately a pore size (e.g., diameter d) because pores are the conduits carrying flow in porous media. On the other hand the appropriate characteristic dimension in *Da* is core length L because reaction occurs along its entire length (Diabira et al. 2001). Notice that in *Da* ratio L/v represents the time for CO_2 to sweep the core sample of length L. The *Pe* and *Da* numbers can then be expressed as follows:

$$Pe = \frac{q\sqrt{k}}{\pi r^2 \phi D} \tag{11}$$

$$Da = \frac{(1-\phi)\,\alpha \pi r^2 L \kappa}{q} \tag{12}$$

where q is Darcy velocity, k is permeability and r is core radius. Since the rate data are usually reported for 25°C, the following equation can be used to obtain the rate constant at a different temperature.

$$\kappa\,(T) = \kappa_{25}\mathrm{Exp}\left[\frac{-E_\mathrm{a}}{R}\left(\frac{1}{T} - \frac{1}{298.15}\right)\right] \tag{13}$$

where $\kappa(T)$ is rate constant at absolute temperature T, κ_{25} is rate constant at 25°C, E_a is activation energy and R is universal gas constant.

As can be seen from the above discussion, the porosity and permeability changes as a result of CO_2 injection strongly depend on the distribution of the rock minerals. Although there are a number of mathematical modeling studies for carbon dioxide (CO_2) injection into aquifer formations, experimental studies are limited and most studies focus on injection into sandstone reservoirs as opposed to carbonate ones. Thus, the aim of this paper is to study the effects of injection of CO_2 into carbonates through CT monitored experiments. One unique nature of the present study is that as opposed to tracking porosity and permeability changes through thin sections, X-ray analysis, etc. CT porosity measurements were used. The paper is divided into two parts: experimental and numerical modeling. The experimental part of this study focuses on the effect of chemical kinetics on change in porosity and permeability of the highly heterogeneous carbonate rocks through injection of gaseous CO_2 in presence of salty water. Effects of flow direction (horizontal or vertical), flow rate (low, medium and high), temperature (low, moderate and high), co-injection of CO_2 with brine and the effect of heterogeneity are discussed. Matches of permeability behavior with the modeling results of a commercial simulator are given in the numerical modeling part.

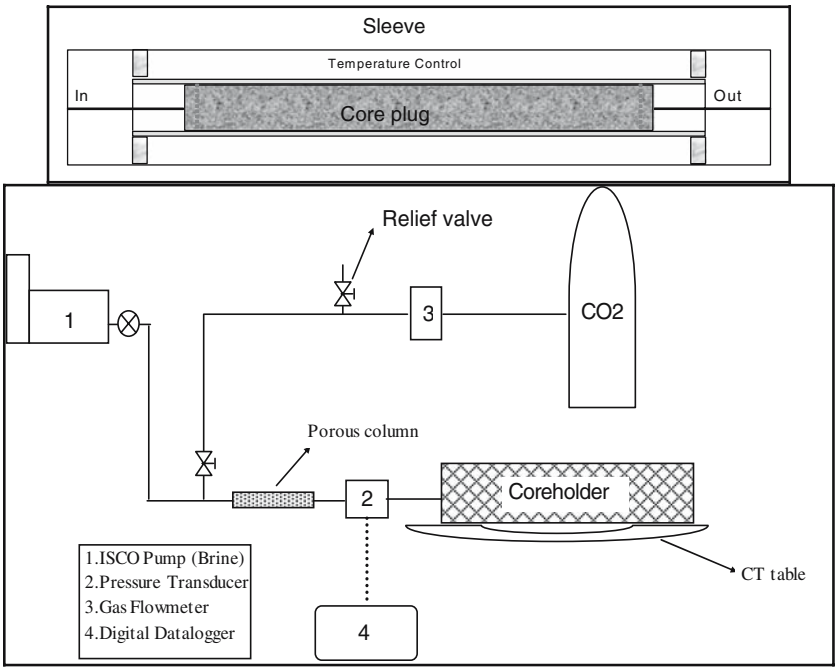

Fig. 1 Experimental apparatus (bottom) and core holder (top) used in the experiments

2 Experimental set-up and procedure

The experimental apparatus consists of, X-ray CT scanner (3rd generation Philips Tomoscan 60/TX), injection system, core holder and data recording system (Fig. 1). The injection system is made up of a constant displacement pump, CO_2 bottle, gas flow meter controller and a pressure transducer. For horizontally aligned experiments a Hassler type X-ray transparent aluminum core holder wrapped with Fiberfrax insulation and carbon fiber materials to minimize X-ray scanning artifacts is used. For vertically oriented experiments a core holder placed in a water jacket that enabled fast adjustment of the system temperature at a constant level was used. Carbonate core plugs drilled from the Midyat formation located in South East Turkey (9 experiments), and homogeneous carbonate core coming from a French quarry, St. Maximin, (1 experiment) were used in experiments. Midyat rock is mainly a heterogeneous carbonate with vugs and fractures. For vertically aligned experiments epoxy coated core plugs of 10.7 cm long and 4.72 cm in diameter were used as opposed to 7 cm long and 3.81 cm ones used in horizontal experiments. Table 1 gives the experimental conditions and physical properties of the core plugs used in the experiments.

The system confining pressure was kept at 3,447.379 kPa (500 psi) using a manually operated hydraulic pump. The temperature of the system was kept at the desired temperature using an electronic temperature controller with an accuracy of 0.1°C and a heating rod. In all experiments prior to start CO_2 was injected into the core plug through a spider web shaped injection port in order to remove possible remaining air trapped in pores. Spider web injection configuration also enabled even distribution of CO_2 at the inlet face of the core plug. Reference dry CT scans (Fig. 2) of eight equally separated volume elements (slices) were acquired and after each CO_2 injection period. Reference dry CT images captured at this stage

Table 1 Experimental conditions and core plugs properties used in the experiments

Experiment	1	2	3	4	5	6	7	8	9	10
Orientation	V	V	H	V	V	V	H	H	H	H
Temperature (°C)	18	18	18	18	18	18	50	35	18	18
Injection rate (cc/min)	3	3	3,6,60	60	60	60	60	6	6	10
Velocity (cm/s) ($\times 10^{-3}$)	2.86	2.86	4.39, 8.77, 87.7	57.2	57.2	57.2	87.7	8.77	8.77	26.7
Salinity (weight % NaBr)	10	10	10	0	2.5	5	10	10	10	20[a]
Diameter (cm)	4.72	4.72	3.81	4.72	4.72	4.72	3.81	3.81	3.81	2.5[b]
Length (cm)	10.7	10.7	7	10.7	10.7	10.7	7	7	7	20
Initial porosity (%)	24	11	22.3	21	26.8	24.4	10	30	17.55	41.7
Initial permeability (md)	44	23.4	451.9	19.9	58.7	38.6	2.9	79	731.9	1020
Heterogeneous	Yes	Yes	Yes	Yes	Yes	Yes	Yes	No	Yes	No
Plugging range, 1/7th (μ)	0.95	0.69	3.04	0.64	1.09	0.89	0.24	1.27	3.86	4.56
Plugging range, 1/3rd (μ)	2.21	1.61	7.09	1.49	2.55	2.07	0.57	2.96	9.02	10.65
Pe	3.10	4.93	16.42	47.67	64.16	57.15	58.66	10.20	53.10	102.12
$Da \cdot Pe$	1.60	2.99	3.70	1.28	1.60	1.47	0.14	0.40	6.34	6.37

V, Vertical; H, horizontal

[a] NaCl

[b] Parallelpiped

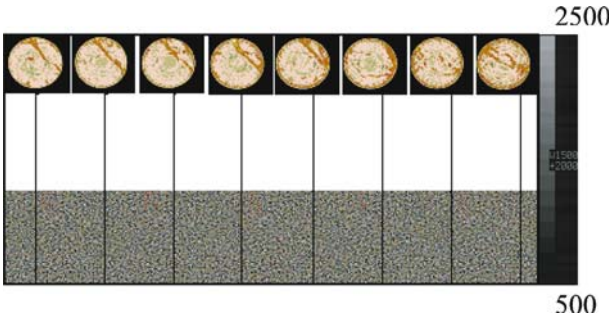

Fig. 2 Raw CT images and their locations along the core plug for experiment 3

were compared to previous ones to ensure no brine is left in the core plug. If the average CT number change for each slice between these scans was more than 5%, CO_2 injection continued. Approximately 10 pore volumes of CO_2 injection ensured the reference dry scans were within the set error limit. At the end of each CO_2 injection period the core plugs were re-saturated with NaBr brine and reference wet CT scans were shot at the same locations when the system reached steady conditions. NaBr brine as opposed to NaCl brine allowed an accurate determination of the porosity (Akin and Kovscek 2003). Porosity of each slice was then obtained by averaging porosities obtained in a circular region of interest that is slightly smaller than the diameter of the core plug. The porosity, ϕ for a slice was obtained using the Eq. 14 (Akin and Kovscek 2003).

$$\phi = \frac{CT_{\mathrm{wr}} - CT_{\mathrm{ar}}}{CT_{\mathrm{w}} - CT_{\mathrm{a}}} \tag{14}$$

where CT_{wr} and CT_{ar} are 100% wet and 100% dry images and CT_w and CT_a are pure fluid CT numbers in Hounsfield units. The distribution of porosities and raw CT images (Fig. 2) showed the heterogeneous nature of the core plugs. Using a data logger pressure readings obtained from a pressure transducer (accuracy 0.1%) were recorded when the brine flow reached steady conditions. Absolute brine permeability at the end of each CO_2 injection period was calculated using the Darcy's law. Breakthrough time and pore volume of the core plug were also determined at this stage. Experiments were conducted at differing injection rates (3, 6 and 60 cc/min), temperatures (18, 35 and 50°C) and brine salinities (0, 2.5, 5 and 10 wt%).

3 Experimental results and discussion

3.1 Effect of flow direction

The results of experiments suggest that orientation of core, which determines the direction of flow, has a crucial role on rock property alteration trends. Generally for vertically oriented core plug experiments the permeability increased and then decreased after a certain pore volume regardless of the salinity and injection rate. On the other hand, for horizontally oriented core plugs the permeability initially decreased and then after a certain injection period then stabilized (Fig. 3).

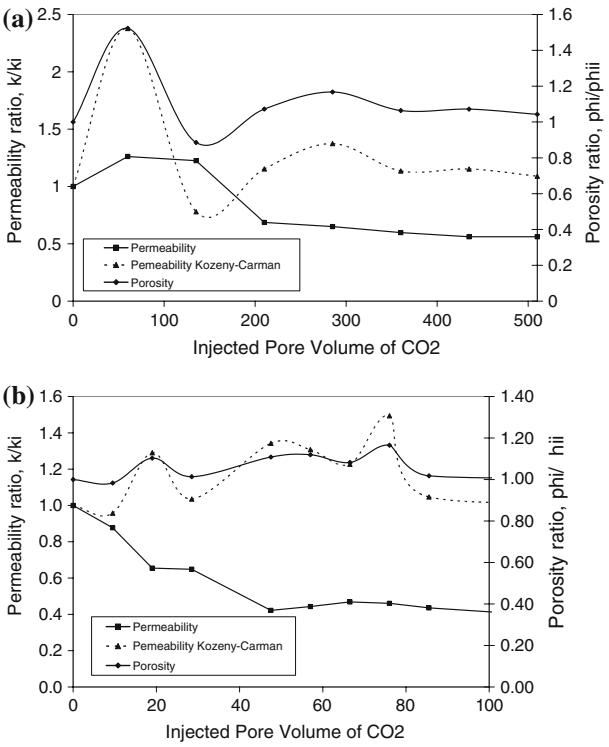

Fig. 3 Effect of orientation (**a**) vertical (experiment #2) and (**b**) horizontal (experiment #3)

Porosity, however, did not exactly match the permeability behavior but showed similar trends. The difference may be due to manner in which particles blocking pore throats. Bridging and plugging can be estimated to occur by two empirical relationships (Hibbeler et al. 2003). If the particle diameter is more than one-half of the pore diameter, then a bridge will form. If the particle diameter is between 1/3rd and 1/7th the size of the pore diameter then it will plug. This process results in a decrease in permeability. Using the relationship that the square root of permeability is approximately equal to pore diameter in microns, plugging range of calcite particles is calculated (Table 1). For heterogeneous Midyat carbonate core plugs the pores and throats have small-to-large values (Fig. 4). Thus, the small calcite particles with a particle diameter between 1 and 2 μ could plug the smaller pores along the flow path for all cores except for the homogeneous core plug. As can be seen in Table 1, *Pe* and *PeDa* numbers can be considered as moderate. At moderate *Pe* and *PeDa* numbers, reactions are generally non-uniform, with more in the upstream and less in the downstream. Thus, a perturbation in the reaction rate at the advancing dissolution front changes the local permeability which in turn affects solute transport and the dissolution rate. As a result, the front becomes unstable and pronounced channels are formed in which most of the flow is focused while most of the pore space is eventually bypassed. Because of the presence of those preferential flow paths, drastic changes in permeability should be expected while only a little change in porosity is observed.

Yet another important issue is mobilization of particles in the porous medium. When the fluid is injected into porous medium and the fluid velocity reaches the particles' mobilization velocity, these particles may move and cause some plugging, hence reduce the permeability of the porous medium. For sand particles with a mean diameter of 2.0–2.5 μm (98% less

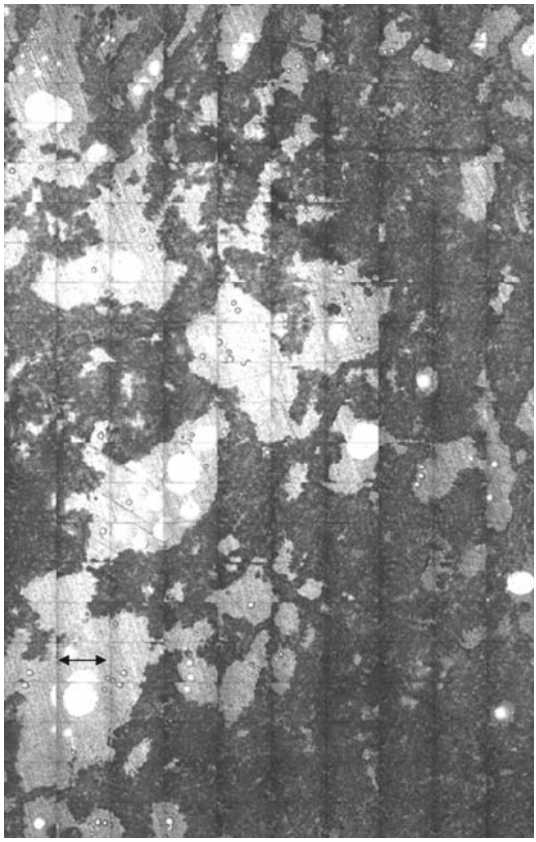

Fig. 4 Thin section image of core plug used in experiment 3. In this image, white areas represent pores. Black arrow is 1 μm long

than 10 μm) Gabriel and Inamdar (1983) found that superficial critical mobilization velocity was 0.007 cm/s for Berea sandstone core plugs. When superficial velocities attained in this study (Table 1) are compared to this critical velocity it can be seen that this value is exceeded for all experiments except for experiments 1–3. As a conclusion calcite dissolution and/or precipitation occur only as a result of CO_2 forming a weak carbonic acid with brine.

In vertically oriented core plugs due to gravitational forces CO_2 easily moves to the top of the core that is identified by early breakthrough times. This in turn increases the contact area of the CO_2 in pores near the inlet and increases chemical reaction frequency. Carbonic acid dissolves pore linings (Zones of accumulation that may be either coatings on a pore surface or impregnations of the matrix adjacent to the pore) of carbonate rocks, and increases the permeability near the inlet (Bjorlykke 1989). As the injection continues some of the precipitated calcite blocks the smaller pores along the flow path. Calcite crystals precipitate in the flow path because of the pressure drop and continuous increase in the amount of dissolved particle, resulting in a decrease in permeability later during the experiment.

On the other hand, for horizontally aligned core plug experiments injected carbon dioxide does not move easily to the end of the core plug and forms carbonic acid near the inlet. Longer breakthrough times compared to vertical cases are observed porosity increases near the inlet only. Calcite then precipitates along the flow path especially near the exit, which decreases porosity. Sample CT derived porosity values support this theory as shown in Fig. 5.

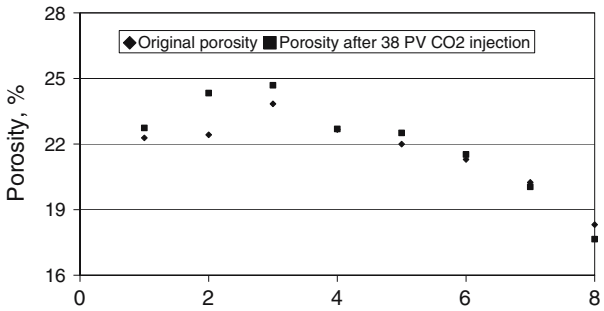

Fig. 5 Porosity change along the core plug observed during experiment 3 (Horizontal, 10% NaBr, 18°C, 3 ml/min)

Similar CT derived porosities were obtained in other experiments. Moreover, a milky fluid is produced from the outlet because of presence of precipitates in the effluent. Continuous measurement of the pH of the produced effluent, which is discussed in following sections, also supports this idea.

3.2 Effect of salinity

It was observed that the salinity (Fig. 6) of the brine has small effect on changes in rock properties as the salinity was increased from 0 to 10% by weight. When distilled water was used, the permeability initially increased by 40%, which was higher when compared to saline cases (20%). As the salt content increased the late time permeability drop was more pronounced. For the experiments in which heterogeneous core plugs were used, because of the possibility of a particle to block a pore throat, permeability decreases as the weight percent of brine increases. These results are sensible. As salinity increases, CO_2 solubility decreases and the strength of the acid decreases as well. Fewer ions in solution mean less dissolution or precipitation.

3.3 Effect of injection rate

Injection rate (Fig. 7) of CO_2 has small effect on changes in rock properties as the injection rate of CO_2 was increased from 3 to 60 ml/min. There are two factors that play a role in the deposition process during particle movement and scaling: the characteristics of the porous medium and the physical and chemical properties of the injection fluid (Moghadasi et al. 2005). For lower flow rates, the rate of precipitation and chance of the particles to block the pore throats increase. As the injected effluent velocity decreases, the plugging rate also increases as a result of clogging constrictions located at the beginning of the flow path. Slow rates also favor the completion of the chemical reactions leading to more precipitation. For the CO_2 injection rate of 3 ml/min (Fig. 7a) 60% decrease in permeability was observed whereas 40% decrease in permeability was detected for the experiment conducted with 60 ml/min injection rate (Fig. 7c). This is expected since for the 60 ml/min experiment critical superficial mobilization velocity is exceeded. For the experiment conducted with flow rate of 6 ml/min (Fig. 7b) a sudden increase in permeability was observed. It may be because of a salt particle blocking the pore throat and then again being released. Also note that for this experiment both the *Pe* and *PeDa* numbers are relatively high compared to other experiments. At high *Pe* and *PeDa* numbers, wormholes are formed and permeability increases greatly due to the dissolution process. As a result, salt concentration of the brine has a stronger effect on permeability reduction than flow rate.

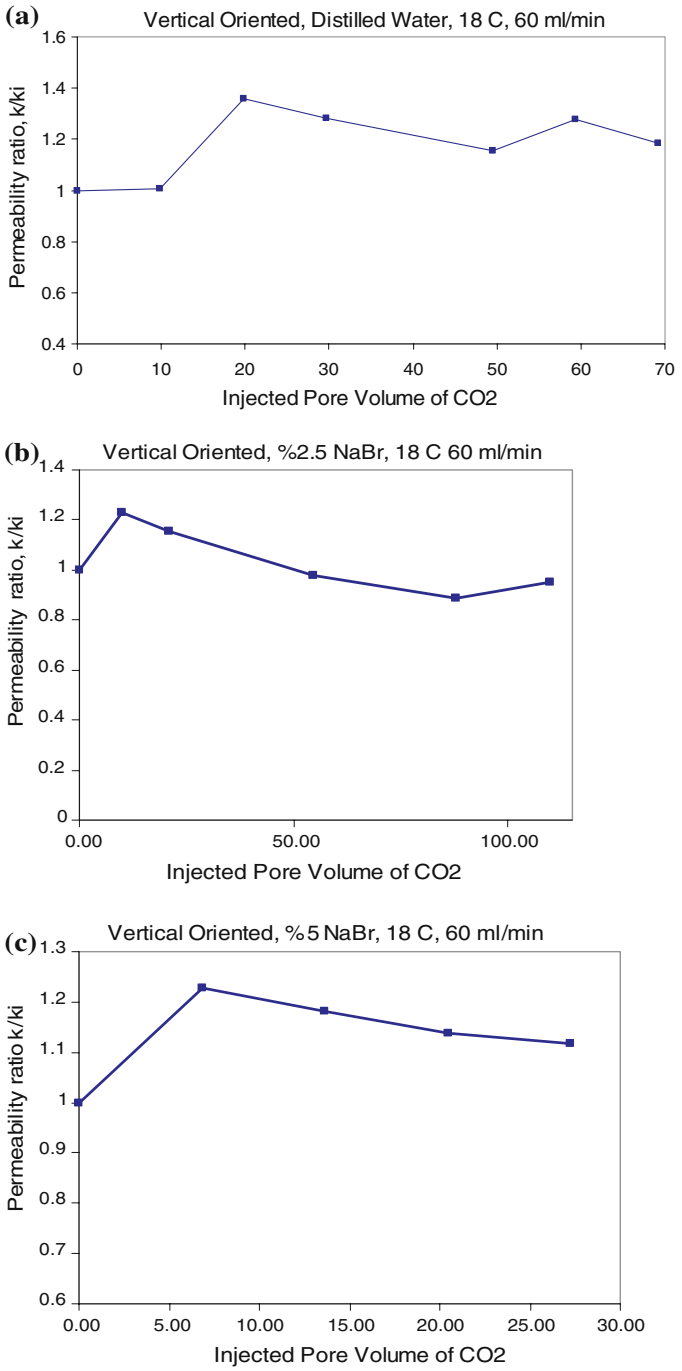

Fig. 6 Effect of salinity: (**a**) distilled water (experiment #4), (**b**) 2.5% NaBr (experiment #5), (**c**) 5% NaBr (experiment #6)

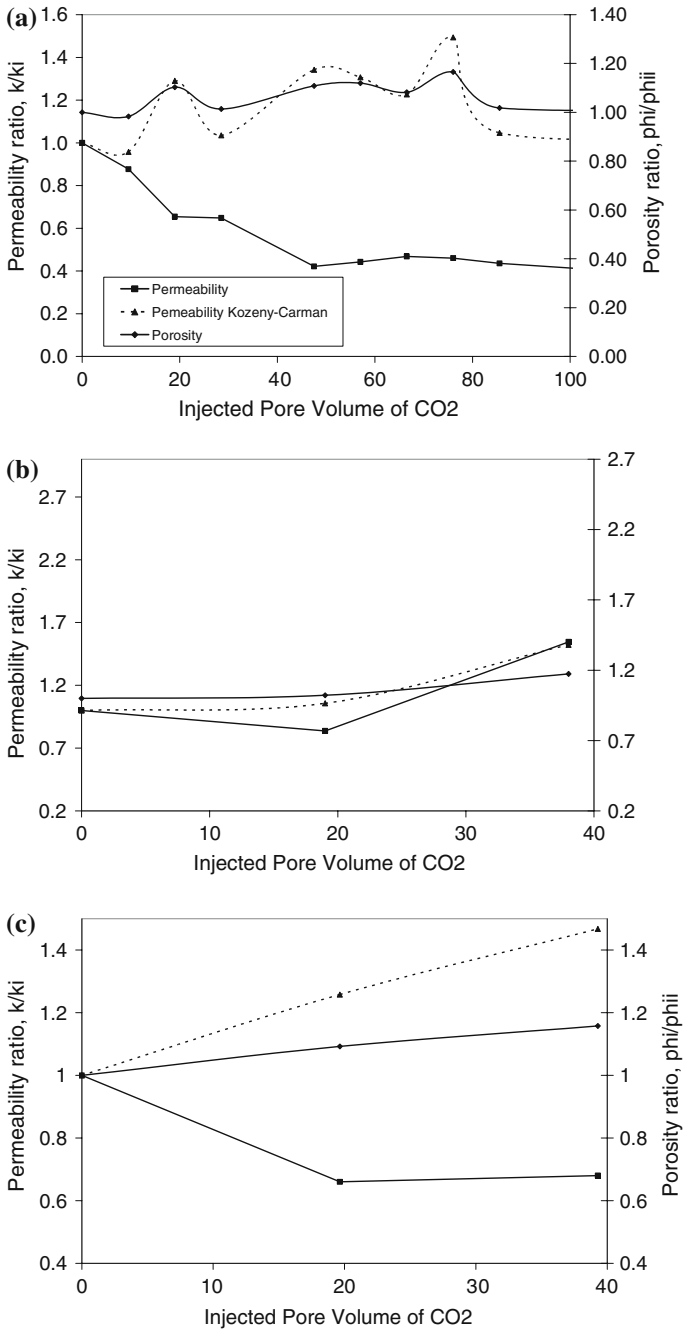

Fig. 7 Effect of injection rate: (**a**) 3, (**b**) 6, (**c**) 60 ml/min (experiment #3)

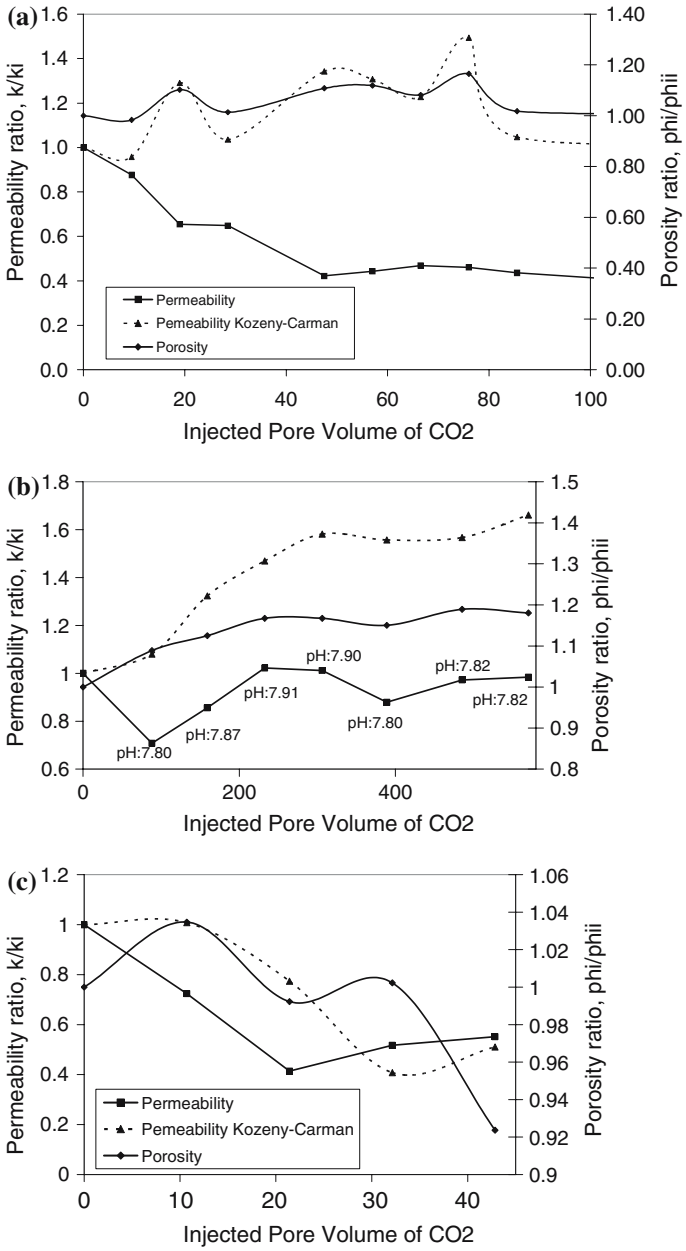

Fig. 8 Effect of temperature: (**a**) 18°C (experiment #3), (**b**) 35°C (experiment #8), (**c**) 50°C (experiment #7)

3.4 Effect of temperature

The solubility of carbon dioxide in water decreases with increase in temperature (Pruess and Xu 2001). Then, a decrease in the temperature of the aquifer would lead to increase in acidity of the aquifer fluid by dissolving more CO_2. An increase in pH should result in more dissolution of rock minerals. The effect of temperature on calcite deposition and porosity and permeability was analyzed using three experiments conducted at 18, 35 and 50°C all using horizontally oriented core plugs (Fig. 8). The last one is a typical temperature observed in shallow geothermal reservoirs. Note that the solubility of calcite decreases with increasing temperature over a portion of the temperature range covered in these experiments. The CO_2 injection rates covered a wide range (3–60 ml/min) corresponding to slow reservoir flows and fast near well bore flows. At 18°C (Fig. 8a), the permeability decreased to 40% of the initial permeability after CO_2 injection and then stabilized around this value for a while. Then it started to decrease again. Due to the fact that the *PeDa* products are small for the high temperature experiments, dissolution or precipitation is relatively uniform compared to low temperature experiments, and these two processes can be approximately reversed by each other. This dissolution and precipitation behavior was also observed for the experiments conducted at lower (18°C) and higher (50°C) temperatures. For the 35°C experiment, permeability initially decreased and then increased. The permeability trend for this experiment followed the porosity trend. The permeability calculated from porosity using a Kozeny–Carman type equation (CMG 2003) (Eq. 15) did not exactly match the observed permeability.

$$k_{\mathrm{f}} = k_0 \left(\frac{\phi}{\phi_0}\right)^c \left(\frac{1-\phi_0}{1-\phi}\right)^2 \tag{15}$$

where k_0 and k_{f} represents the initial and final permeabilities, ϕ_0 is the initial porosity and c is the Kozeny–Carman coefficient. Kozeny–Carman type equations were previously used by McCume et al. (1979), Itoi et al. (1987) and Lichtner (1996). Pange and Ziauddin (2005) used a modified Kozeny–Carman approach to model experimental dissolution patterns observed in carbonates during acidizing process. The application of Eq. 15 with exponents 3.0, 5.0 and 12.0 delineates the possible range of k–ϕ relations (Kühn 2004). The exponent 3.0 represents clean formations with relatively smooth shaped grains. An exponent of approximately 5.0 has been determined for anhydrite precipitation found in rock samples of deep geothermal aquifers from northern Germany. The mineral deposit developed in this case on geological time scales. On the contrary, an exponent of 12.0 has been determined in core flooding laboratory experiments, representing the technical time scale, where anhydrite re-located (dissolved and subsequently precipitated) within a temperature front (Bartels et al. 2002). Note that permeability calculated from porosity using Kozeny–Carman type of equation assumes that tortuosity is constant. In practice, however, as carbonic acid dissolves calcite and then precipitates again, the tortuosity should change continuously. In Kozeny–Carman's and other classic models (e.g., Walsh and Brace (1984)), permeability is described as proportional to simple integer powers of the relevant pore geometry parameters. For a given process, these parameters are usually assumed to be related to each other through power-law relationships, therefore leading to a power-law dependence of permeability on porosity, possibly with a non-integer exponent (e.g., David et al. 1994). Experimental evidence, however, indicates that a single power-law exponent does not always hold as porosity changes. One popular approach is to keep the power-law representation but with a variable exponent (Bernabe et al. 2003). Accordingly, we depict the evolution of permeability and porosity in carbonates as a result of CO_2 injection as oriented lines in log (porosity)–log (permeability) space through

time. The slope of the tangent at any point on such a curve can be understood as the exponent of a local power-law $k \propto \phi^c$, where k is the permeability and ϕ the porosity. Our assumption here is that c is related to changes in the ratio of effective over non-effective porosity in carbonates. Moreover, for the experiments where the Kozeny–Carman type model represents the permeability change it could be speculated that the tortuosity does not change or stays nearly constant.

The pH analysis of the produced effluent for the 35°C experiment showed that right after CO_2 injection pH of the effluent became basic (pH: 7.90). With more injection of CO_2, some decrease in pH (pH: 7.80) was observed (Fig. 8b). Since chemical interaction between CO_2 and brine results in formation of carbonic acid a decrease in pH is expected. In essence the pH of the effluent closely followed the permeability and porosity change. It is known that an increase in the total amount of calcite leads to increase in pH (Omole and Osaba 1983). Soong et al. (2004) studied the reaction of CO_2 with brine samples collected from the Oriskany Formation in Indiana County, PA, in an autoclave reactor under various conditions. The combined experimental and modeling data suggested that pH (pH > 9) plays a key role in the formation of carbonate minerals. Moreover, they have stated that the effects of temperature and CO_2 pressure have a lesser impact on the formation of carbonate minerals.

3.5 Effect of heterogeneity

We used a homogeneous carbonate core plug coming from a French quarry (St. Maximin). This carbonate is known to be quite homogeneous with high porosity and permeability (0.417 and 1.02 Darcy, respectively). The core has parallelepiped shape ($5 \times 5 \times 20\,cm^3$) and was placed vertically in a core holder. The experiment was conducted using distilled water pre-saturated with CO_2 introduced from the bottom of the core plug. Permeability continuously increased following the CO_2 injection (Fig. 9). Dissolution of the carbonate rock by CO_2 is shown through permeability change (45%) but porosity increase (from 0.417 to 0.432) was not so high. From these results it can be seen that the rock is not dissolved in a continuous way but that preferential channels (wormholes) are generated in the rock. Assuming the pore size distribution is uni-modal and that the pores and pore throats are evenly distributed and large, it could be speculated that the calcite particles never find a chance to deposit along the core. On the other hand for heterogeneous carbonate core plugs, because the pore size distribution is bimodal and the pores and throats have small to large values, the calcite particles could deposit along the flow path. Thus, the process strongly depends on pore size distribution and the injectivity will greatly change as a result. Similar results have been reported in the literature (Ross et al. 1982).

3.6 Effect of injecting CO_2-saturated brine

During the CO_2 injection process, at some point in the reservoir, CO_2 saturated brine may flow. In order to simulate this behavior 10% NaBr brine was saturated with CO_2 and the resulting fluid was injected into a core plug placed horizontally in the core holder in a similar fashion (See experiment 9 in Table 1). The experiment mimicked other horizontal experiments. There was an initial decrease in permeability followed by an oscillatory behavior (Fig. 10). The porosity decreased and then increased as the injection continued. When compared to other horizontal experiments it could be seen that the results are in agreement. Thus, the same chemical and physical forces are in action.

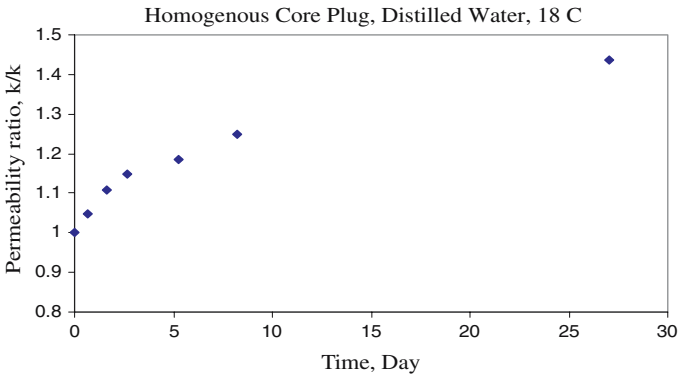

Fig. 9 Permeability change observed during experiment #10 (homogeneous carbonate core plug)

Fig. 10 Permeability change observed during co-injection of CO_2 and brine (experiment #9)

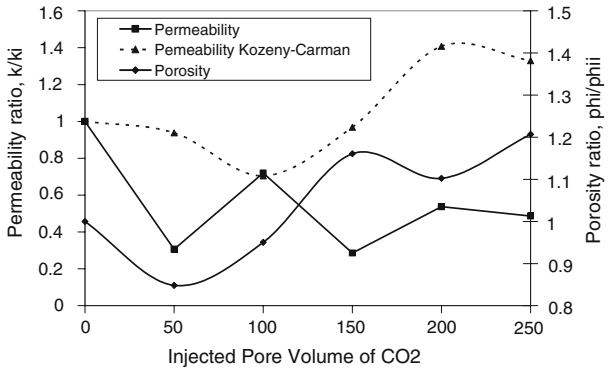

3.7 Supercritical CO_2 injection

Geologic disposal of CO_2 into aquifers would be made at supercritical pressures, in order to avoid adverse effects from CO_2 separating into liquid and gas phases in the injection system. Only a few studies do examine reactions in host rock in response to addition of CO_2 under supercritical conditions. In geochemical modeling studies that incorporate kinetic rate laws (Perkins and Gunter 1995; Gunter et al. 2000) and one study combining experiment and modeling (Gunter et al. 1997), dissolution of silicate minerals in a brine and precipitation of carbonate are reported. In the latter study, however, experiments consisted of month-long batch reactions at 105°C and 90 bars in which no silicate dissolution textures or new major reaction products were observed. With few exceptions (i.e., Gunter et al. 1997; Kaszuba and Janecky 2000; Kaszuba et al. 2001, 2003), there is no published experimental evaluation of geochemical reactions that occur within a supercritical CO_2–brine–aquifer system at reservoir temperature and pressure. For supercritical CO_2 injection at 200°C and 200 bars, Kaszuba et al. (2003) reported that the reaction among supercritical CO_2, brine and rock exhibits relatively rapid kinetics that are similar to rates measured in systems where gaseous CO_2 is injected. Based on the observations from the previous section on injecting CO_2-saturated brine, one would expect that supercritical CO_2 injection will produce similar results to those presented in this study, but further research is required to verify this conclusion.

3.8 Core-scale numerical model

Early studies relating porosity-permeability changes under consideration of reactive transport processes are rare, but this field of research is developing during the last decade. Zarrouk and O'Sullivan (2001) gave a review of the effect of chemical reactions on the porosity of a porous medium and resulting permeability changes. They concluded that every simulation code for reactive transport should be adaptable concerning the applied porosity–permeability relationships, thus, it is possible to use any relation. The simulator Processing SHEMAT/SHEMAT (Clauser 2003) is an example, where varying relationships can be applied. The simulator codes CHEM-TOUGH and TOUGH/EWASG (Pruess and Xu 2001) are further examples of reactive transport models applicable to systems in which permeability changes resulting from chemical reactions are considered. In CHEM-TOUGH permeability is assumed to vary with porosity according to the Kozeny–Carman power of three, whereas in TOUGH/EWASG the permeability change is far more complex. TOUGH/EWASG provides the opportunity to calculate permeability changes based on either a straight capillary tube model, or a model consisting of alternating segments of capillary tubes with larger and smaller radii, or for parallel-plate fracture segments of different aperture in series (Pruess and Xu 2001). The first model simplifies to a relationship in which permeability varies with porosity to the power of two. The models of "tubes in series" and "fractures in series" depend on additional parameters beside porosity and permeability and are therefore not discussed here. Yet another code that can simulate porosity and permeability modification as a result of CO_2 injection is PHREEQC (Parkhurst and Appelo 1999).

In this study, STARS (CMG 2003) a new generation advanced processes and thermal reservoir simulator was used. STARS is capable of simulating many types of chemical additive processes, using a wide range of grid and porosity models at both laboratory and field scales. In all simulations, a radial grid block system with $14 \times 25 \times 24$ (r, θ, z) blocks was used to model the laboratory experiments. Initial porosities obtained from CT scans were designated to each grid block corresponding to a slice (Fig. 11). The missing porosities in between the slices were distributed using an inverse-distance squared distribution function. Initial permeabilities of each grid were assumed constant. Brooks–Corey CO_2–water relative permeabilities and Brooks–Corey capillary pressures (pore size distribution index, $\lambda = 0.4$, entry capillary pressure, $P_d = 0.11$ MPa, irreducible water saturation, $S_{wirr} = 0.13$) were used. Note that low pore size distribution index indicates greater heterogeneity. CO_2 is defined as real gas and CO_2 solubility in water is taken to be proportional to CO_2 partial pressures at pressures of a few bars, but increases only very weakly with pressure beyond 100 bars (Spycher et al. 2003). Langmuir type adsorption of CO_2 was also considered. The dissolution and precipitation reactions given by Eq. 1–5 were treated separately. The reaction model's heterogeneous mass transfer (source and sink) terms were applied to the non-equilibrium capture and release of calcite by the porous rock. This requires that the reaction rate constants depend on permeability to account for the changes in capture efficiency as the calcite particle size to pore throat size ratio changes. To specify the dependence of chemical reactions and non-equilibrium mass transfer on permeability (10, 20, 750 and 1000 md) an effective permeability reaction rate scaling factor (2.5, 1.0, 0.75 and 0.5 min^{-1}) table was used. Thus, permeability change was controlled by reaction frequencies (1/min kPa) of the dissolution and deposition reactions and a variable Kozeny–Carman coefficient given by Eq. 15. The details of the numerical model can be found elsewhere (Izgec et al. 2007).

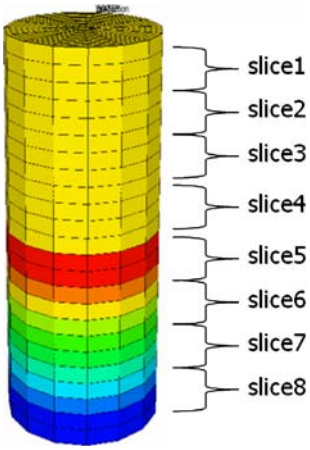

Fig. 11 Distribution of slice porosities in core-scale model

3.9 Results and discussion of numerical simulation

In order to show that the model could be used to simulate the experiments a synthetic case similar to experiments 1 was used. In this simulation, CO_2 was injected in a continuous manner (3.0 cm^3/min) from the bottom face of the numerical model to mimic the vertical-flow experiments. Initial horizontal and vertical permeabilities were constant: 90 and 20 md, respectively. Initial effective porosity was 23.8%. The core outlet pressure was 101 kPa at 21°C. It was observed that chemical reactions occurred preferentially in the center of the core where CO_2 injection is performed (Fig. 12). At this location, the sizes of the grid blocks are relatively smaller than the ones located near the borders. Dissolution and increase in permeability were observed especially at the inlet of the core plug while at some grid blocks permeability impairment was observed. At the bottom and the top of the core, some permeability decreases were also noted. As the injection continued, CO_2–rock–brine interaction resulted in various non-uniform dissolution patterns and in some cases to re-precipitation and permeability reduction. Thus, it is an unstable dissolution process leading to different dissolution regimes. This unstable dissolution process results in preferential flow patterns so-called wormholes that can be visualized in Fig. 12 along the center of the core as discussed before.

A cutting plane at the middle of the core was used to examine the profiles on a vertical plane (Fig. 12). Injected CO_2 moved toward to top of the core while some amount was dissolved in brine. Figure 12 shows the vertical movement of gaseous CO_2, caused by buoyancy forces, and time-dependent gas saturation distribution. It could be seen that after the vertical movement, free phase gas accumulated at the upper part of the core for a while. Then, CO_2 started to dissolve into water. Thus, gas saturation at the top portion of the core decreased. It is known that dissolution of CO_2 into water increases the density of the brine. Change in water density observed in the simulation agrees with the theory. Water density increases with time as free phase gas amount decreases. As the free phase gas at the upper portion of the core dissolved into brine, density of the fluid increased and started to migrate downwards and was replaced by unsaturated brine. Results of core-scale simulation reveal that adsorption of CO_2 onto carbonate rock surface is less pronounced compared to other trapping mechanisms. Adsorption of CO_2 takes place where CO_2 is in free gas phase. The concentration of bicarbonate ions in brine with time in the core plug continuously increased (Fig. 12). This means dissolution takes place at the flow path of the CO_2, especially near the inlet. These results are in accord with aforementioned experimental observations.

Fig. 12 Time dependent (**a**) permeability (md) change, (**b**) CO_2 saturation evolution, (**c**) brine density (kg/cm^3) change, (**d**) adsorbed CO_2 (ppm) and (**e**) concentration of bicarbonate (g mol/cm^3) (bottom). Model results of experiment 3 at 10, 30, 65, 105, 145 and 180 min (left-to-right of each image)

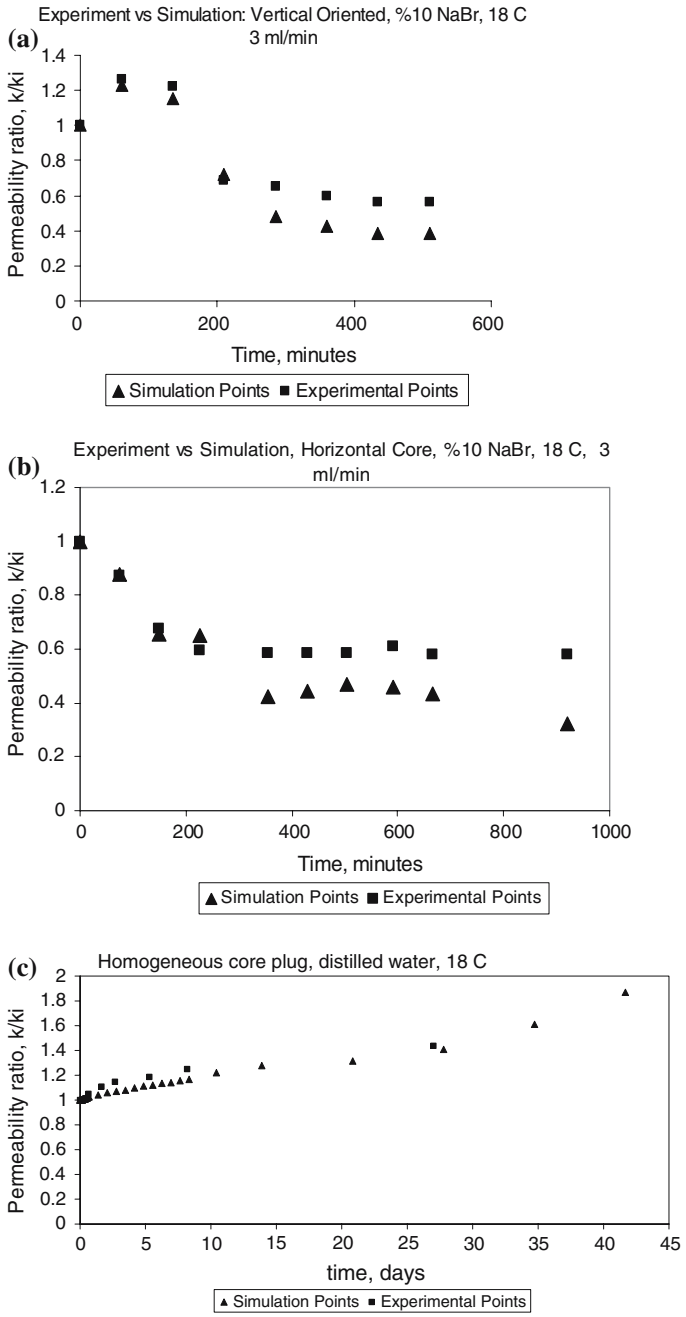

Fig. 13 Comparison of experimental and model permeability changes: top: #1, middle: #3, bottom: #10

Calibration of the simulation model was conducted by changing the following parameters: the reaction frequencies of the dissolution and deposition reactions (Eqs. 1–5), and the Kozeny–Carman coefficient (c in Eq. 15). Reaction rate scaling factor, blockage effect

of particles, adsorption rate of CO_2 and initial concentrations of solid phase carbonate and aqueous phase bicarbonate and aqueous phase NaBr were set to experimentally observed values. It was observed that matches could be obtained by setting forward and backward reaction frequencies to 3,500 and 550 and Kozeny–Carman coefficient to 6.5. For vertical experiments the initial concentration of the dissolved bicarbonate (1 gmol/cm^3) was 10 times higher compared to horizontal cases. Figure 13 gives the comparison of experimental and numerical permeability values for vertical and horizontal oriented heterogeneous and vertical oriented homogenous core plug experiments with varying conditions. Results show that composition of the fluids initially present in the core plug and reaction frequencies of the reactions play important roles in fluid–rock–gas interaction leading to changes in rock properties. Blockage effect of calcite and salt particles also play a major role in porosity and permeability alteration trend.

The results shown here, derived from an empirical comparison between experimental measurements on very simple plug-scale samples and simulations obtained with a reaction-transport code, indicate that the problem is far from being straightforward. A non-empirical approach would be to consider the mass-balance equations of the reaction-transport problem at the pore scale, and to integrate them at the scale of a representative elementary volume (a scale where the Darcy's law would be used), using a methodology developed for instance by Quintard and Whitaker (1999). This approach is beyond the scope of the present paper.

It should be also noted that injection of CO_2 into a saline aquifer for sequestration is a two-phase flow condition. Relative permeability and residual CO_2 saturation are the salient properties that influence sequestration under this condition. Drainage relative permeability controls the ability of CO_2 to flow into the aquifer (i.e., The saturation range for which the CO_2 plume is mobile is given by relative permeability curves.) as it is being injected, and residual saturation dictates the volume of CO_2 held immobile in the aquifer by capillary forces after injection. In the context of CO_2 sequestration the most favorable geologic situation is to optimize the relative permeability effects to enhance injection while maximizing the residual CO_2 saturation. A dependency was reported by Holtz (2003) between rock quality and end-point relative permeability saturations and the crossover point between phases. He also reported that decreasing rock quality was shown to increase residual saturation.

As discussed earlier in this section, the results shown here are derived from an empirical comparison between experimental measurements on very simple plug-scale samples and simulations obtained with a reaction-transport code. This indicates that the problem is far from being straightforward. It is possible to improve the matches reported here by modifying certain rock properties like water–CO_2 drainage relative permeabilities and capillary pressures. No attempt was made to enhance the matches by varying properties such as relative permeability. That is why the numerical solutions discussed in this section should be used as guidelines rather than to the point results. Nevertheless, the current configuration enables the numerical model match the experimental results.

4 Conclusions

Results of this study show that:

1. The trend of change in rock properties as a result of injection of CO_2 into carbonate formations, is very case dependent because it is related to distribution of pores, brine composition and as well the thermodynamic conditions. From the results presented it can be inferred that the rock is not dissolved in a continuous way but that preferential channels (wormholes) are generated in the rock (see Table 1 and Figs. 3 and 5).

2. Calcite deposition is mainly influenced by flow direction and horizontal flow resulted in larger calcite deposition compared to vertical flow (Fig. 3).
3. For the temperature range studied (18–50°C) permeability and porosity alteration trends did not change (Fig. 8).
4. Mineral trapping of CO_2 is less pronounced compared to other trapping mechanisms.
5. A continuous change of injectivity was observed during the injection of CO_2 into carbonate formations because of the chemical kinetics and accompanying rock properties' alterations (Fig. 10).
6. Composition of the fluids initially present in the core plug and reaction frequencies of the reactions play important roles in fluid–rock–CO_2 interaction leading to change in rock properties (Fig. 6).
7. A numerical model that considers adsorption of CO_2, solution and dissolution reactions observed in carbonates can simulate injection of CO_2 in carbonate formations.

References

Akin, S., Kovscek, A.R.: Computed tomography in petroleum research. In: Mees, F., Swennen, R., Van Geet, M., Jacobs P. (eds.) Application of X-ray Computed Tomography in the Geosciences, pp. 23–38. Geological Society of London (2003)

Bachu, S., Adams, J.J.: Sequestration of CO_2 in geological media in response to climate change: capacity of deep saline aquifers to sequester CO_2 in solution. Energy Convers. Manage. **44**, 3151–3175 (2003)

Bartels, J., Kühn, M., Schneider, W., Clauser, C., Pape, H., Meyn, V., Lajczak, I.: Core flooding laboratory experiment validates numerical simulation of induced permeability change in reservoir sandstone. Geophys. Res. Lett. **29**(9), 10.1029/2002GL014901 (2002)

Bekri, S., Thovert, J.F., Adler, P.M.: Dissolution of porous media. Chem. Eng. Sci. **50**, 2765–2791 (1995)

Bernabe, Y., Mok, U., Evans, B.: Permeability–porosity relationships in rocks subjected to various evolution processes. Pure Appl. Geophys. **160**, 937–960 (2003)

Bhat, S.K., Kovscek, A.R.: Statistical network theory of silica deposition and dissolution in diatomite. In Situ **23**, 21–53 (1999)

Bjorlykke, K.: Sedimentology and Petroleum Geology. Springer-Verlag, New York (1989)

Clauser, C. (ed.): Numerical Simulation of Reactive Flow in Hot Aquifers using SHEMAT/Processing Shemat. Springer Verlag, Heidelberg-Berlin (2003)

Computer Modeling Group (CMG): CMG STARS User's Guide. Computer Modeling Group Ltd., Calgary, Alberta, Canada (2003)

David, C., Wong, T.-F., Zhu, W., Zhang, J.: Laboratory measurement of compaction-induced permeability change in porous rock: implications for the generation and maintenance of pore pressure excess in the crust. Pure Appl. Geophys. **143**, 425–456 (1994)

Diabira, I., Castanier, L.M., Kovscek, A.R.: Porosity and permeability evolution accompanying hot fluid injection into diatomite. Petrol. Sci. Technol. **19**(9&10), 1167–1185 (2001)

Doughty, C., Pruess, K.: Modeling supercritical carbon dioxide injection in heterogeneous porous media. Vadose Zone Journal. **3**(3), 837–847 (2004)

Gabriel, G.A., Inamdar, G.R.: An experimental investigation of fines migration in porous media. SPE 12168, 58th Annual Technical Conference and Exhibition, San Francisco, CA, October 5–8 (1983)

Goldberg, P., Chen, Z.-Y., O'Connor, W., Walters, R., Ziock, H.: CO_2 mineral sequestration studies in US. In: Proceedings of the First National Conference on Carbon Sequestration, Washington, DC, U.S.A., May 14–17 (2001)

Gunter, W.D., Perkins, E.H., Hutcheon, I.: Aquifer disposal of acid gases: modelling of water–rock reactions for trapping of acid wastes. Appl. Geochem. **15**, 1085–1095 (2000)

Gunter, W.D., Perkins, E.H., McCann, T.J.: Aquifer disposal of CO_2-rich gases: reaction design for added capacity. Energ. Convers. Manage. **37**, 1135–1142 (1993)

Gunter, W.D., Wiwchar, B., Perkins, E.H.: Aquifer disposal of CO_2-rich greenhouse gases: extension of the time scale of experiment for CO_2-sequestering reactions by geochemical modelling. Mineral. Petrol. **59**, 121–140 (1997)

Hibbeler, J., Garcia, T., Chavez, N.: An integrated long term solution for migratory fines damage. SPE Latin American and Caribbean Petroleum Engineering Conference, Port of Spain, Trinidad, West Indies, 27–30 April (2003)

Holtz, H.M.: Pore-scale influences on saline aquifer CO_2 sequestration. AAPG 2003 Meeting, Salt Lake City, Utah, May 11–14 (2003)

Hovorka, S.D., Benson, S.M., Doughty, C., Freifeld, B.M., Sakurai, S., Daley, T.M., Kharaka, Y.K., Holtz, M.H., Trautz, R.C., Nance, H.S., Myer, L.R., Knauss, K.G.: Measuring permanence of CO_2 storage in saline formations -the Frio experiment. Environ. Geosci. **13**, 105–121 (2006)

Itoi, R., Fukuda, M., Jinno, K., Shimizu, S., Tomita, T.: Numerical analysis of the injectivity of wells in the Otake geothermal field, Japan. In: Proceedings 9th New Zealand Geothermal Workshop, November 4–6, Geothermal Institute, University of Auckland, Auckland, New Zealand, pp. 103–108 (1987)

Izgec, O., Demiral, B., Bertin, H., Akin, S.: Calcite precipitation in low temperature geothermal systems: an experimental approach. In: 30th Workshop on Geothermal Reservoir Engineering, Stanford University, Stanford, California, TR-176 (2005a)

Izgec, O., Demiral, B., Bertin, H., Akin, S.: CO_2 injection in carbonates. In: SPE Western Regional Meeting, Irvine, CA, USA, SPE Paper 93773 (2005b)

Izgec, O., Demiral, B., Bertin, H., Akin, S.: Experimental and numerical investigation of carbon sequestration in deep saline aquifers. In: SPE/EPA/DOE Exploration and Production Environmental Conference, Galveston, Texas, SPE Paper 94697 (2005c)

Izgec, O., Demiral, B., Bertin, H., Akin, S.: CO_2 injection into saline carbonate aquifer formations II: comparison of numerical simulations to experiments Transport Porous Media (to appear) (2007)

Johnson J.W., Nitao J.J., Morris J.P.: Reactive transport modeling of cap rock integrity during natural and engineered CO_2 sequestration. Abstr. Pap. Am. Chem. S., **226**: U604-U604 137-GEOC Part 1. (2003)

Kaszuba, J.P., Janecky, D.R.: Experimental hydration and carbonation reactions of MgO: a simple analog for subsurface carbon sequestration processes. Geol. Soc. Am., Abstr. with Prog. **32**, A202 (2000)

Kaszuba, J.P., Janecky, D.R., Snow, M.G.: Carbon dioxide reaction processes in a model brine aquifer at 200 C and 200 bars: implications for subsurface carbon sequestration. Geol. Soc. Am., Abstr. with Prog. **33**, A232 (2001)

Kaszuba, J.P., Janecky, D.R., Snow, M.G.: Carbon dioxide reaction processes in a model brine aquifer at 200°C and 200 bars: implications for geologic sequestration of carbon. Appl. Geochem. **18**, 1065–1080 (2003)

Kumar, A., Ozah, R., Noh, M., Pope, G.A., Bryant, S., Sepehrnoori, K., Lake, L.W.: Reservoir simulation of CO_2 storage in deep saline aquifers. SPE J. 10 (3): 336–348 (2005)

Kühn, M.: Reactive flow modeling of hydrothermal systems. Lect. Notes Earth Sci. **103**, 209–226 (2004)

Lichtner, P.C.: Continuum formulation of multicomponent – multiphase reactive transport. Rev. Mineral. Geochem. **34**(1), 83–129 (1996)

McCume, C.C., Forgler, H.S., Kline, W.E.: An experiment technique for obtaining permeability–porosity relationship in acidized porous media. Ind. Eng. Chem. Fundam. **18**(2), 188–192 (1979)

McPherson, B.J.O.L., Lichtner, P.C.: CO_2 sequestration in deep aquifers. In: Proceedings of the First National Conference on Carbon Sequestration, Washington, DC, U.S.A., May 14–17 (2001)

Moghadasi, J., Müller-Steinhagen, H., Jamialahmadi, M., Sharif, A.: Model Study on the kinetics of oil formation damage due to salt precipitation from injection. J. Petrol. Sci. Eng. **46**(4), 299–299 (2005)

Nghiem, L., Sammon, P., Grabenstetter, J., Ohkuma, H.: Modeling CO_2 storage in aquifers with a fully-coupled geochemical EOS compositional simulator. SPE 89474-MS, SPE/DOE Symposium on Improved Oil Recovery, Tulsa, Oklahoma., April 17–21 (2004)

Nordbotten, M.J., Celia, A.M., Bachu, S.: Injection and storage of CO_2 in deep saline aquifers: analytical solution for CO_2 plume evolution during injection. Transport Porous Media **58**(3), 339–360 (2004)

Omole, O., Osoba, J.S.: Carbondioxide–dolomite rock interaction during CO_2 flooding process. In: 34th Annual Technical Meeting of the Petroleum Society of CIM, Canada (1983)

Pange, M.K.R., Ziauddin, M.: Two-scale continuum model for simulation of wormholes in carbonate acidization. AIChE J. **51**(12), 3231–3248 (2005)

Parkhurst, D.L., Appelo, C.A.J.: User's guide to PHREEQC (Version 2) – a computer program for speciation, batch-reaction, one-dimensional transport, and inverse geochemical calculations: U.S. Geological Survey Water-Resources Investigations Report 99-4259, 312 pp (1999)

Perkins, E.H., Gunter, W.D.: Aquifer disposal of CO_2-rich greenhouse gasses: modelling of water–rock reaction paths in a siliciclastic aquifer. In: Kharaka, Y.K., Chudaev, O.V. (eds.) Proceedings of the 8th International Symposium on Water–Rock Interaction, pp. 895–898 (1995)

Pruess, K., Xu, T.: Numerical modeling of aquifer disposal of CO_2. In: SPE/EPA/DOE Exploration and Production Environmental Conference, San Antonio, Texas, SPE Paper 83695 (2001)

Pruess, K., Xu T.F., Apps, J., Garcia, J.: Numerical modeling of aquifer disposal of CO_2. SPE J. **8**(1), 49–60 (2003)

Quintard, M., Whitaker, S.: Dissolution of an immobile phase during flow in porous media. Ind. Eng. Chem. Res. **38**, 833–844 (1999)

Reichle, D., Houghton, J., Benson, S., Clarke, J., Dahlman, R., Hendrey, G., Herzog, H., Hunter-Cevera, J., Jacobs, G., Judkins, R., Kane, B., Ekmann, J., Ogden, J., Palmisano, A., Socolow, R., Stringer, J., Surles, T., Wolsky, A., Woodward, N., York, M.: Carbon Sequestration Research and Development, Office of Science, Office of Fossil Energy, U.S. Department of Energy (1999)

Ross, G.D., Todd, A.C., Tweedie, J.A., Will, A.G.S.: The dissolution effects of CO_2–brine systems on the permeability of U.K. and North Sea Calcareous Sandstones. In: Proceedings of Society of Petroleum Engineers/U.S. Department of Energy Third Joint Symposium on Enhanced Oil Recovery, Paper SPE/DOE 10685, pp. 149–154 (1982)

Saripalli, P., McGrail, P.: Semi-analytical approaches to modeling deep well injection of CO_2 for geological sequestration. Energy Convers. Manage. **43**, 185–198 (2002)

Snoeyink, L.W., Jenkins, D.: Water Chemistry, pp. 85–135. John Wiley & Sons Publications (1980)

Spycher, N., Pruess, K., Ennis-King, J.: CO_2–H_2O mixtures in the geological sequestration of CO_2. I. Assessment and calculation of mutual solubilities from 12 to 100°C and up to 600 bar. Geochim. Cosmochim. Acta **67**(16), 3015–3031 (2003)

Soong, Y., Goodman, A.L., McCarthy-Jones, J.R., Baltrus, J.P.: Experimental and simulation studies on mineral trapping of CO_2 with brine. Energy Convers. Manage. **45**, 1845–1859 (2004)

Walsh, J.B., Brace, W.F.: The effect of pressure on porosity and the transport properties of rocks. J. Geophys. Res. **89**, 9425–9431 (1984)

Zarrouk, S.J., O'Sullivan, M.J.: The effect of chemical reactions on the transport properties of porous media. In: Simmons, S., Dunstall, M.G., Morgan, O.E. (eds.) Proceedings 23rd New Zealand Geothermal Workshop, November 7–9, Auckland University, New Zealand, pp. 231–236 (2001)

Zhang, D., Kang, Q.: Simulation of coupled flow, transport, and reaction in porous media by lattice Boltzmann method. In: 2004 AGU Fall Meeting, San Francisco, U.S.A. H32A-06 (2004)